Rev. Roum. Sci. Techn.– Électrotechn. et Énerg.
Vol. **64**, *4*, pp. 341–348, Bucarest, 2019

OPTIMAL CONTROLLERS DESIGN FOR ISOLATED HYBRID WIND-DIESEL POWER SYSTEM USING BEE ALGORITHM

WICHAN SRISUWAN[1], WORAWAT SA-NGIAMVIBOOL[1]

Key words: Bee algorithm, Fuzzy logic controller, Load frequency control, Proportional-integral-derivative (PID) controller, Superconducting magnetic energy storage (SMES), Wind-diesel power system.

For this research, the method for applying bee algorithm (BA) to design the optimal controller is presented, *i.e.* scaling factor-fuzzy logic-PID (SF-FLPID), superconducting magnetic energy storage (SMES), and proportional-integral-derivative (PID) controllers. These controllers are used for load frequency control (LFC) of an isolated hybrid wind-diesel (IHWD) power system. Conventionally, the PID controller gains, scaling factor, membership functions (MF), control rules (CR) and PID gains of SF-FLPID controller and the SMES controller gains are derived by trial-and-error processes or the experiences of designers. However, in this research, BA is applied to the control system so that these parameters can be tuned simultaneously and help minimize system frequency deviations against disturbances and variation. Results of simulation explicitly show that the BA approach can achieve high performance for the optimal PID, SF-FLPID and SMES controllers.

1. INTRODUCTION

The hybrid electrical power systems are widely used for electrical power generation since they are independent of a large, centralized electricity grid and comprise of many types of renewable power sources (wind turbine, photovoltaic panels).

Nowadays, the isolated hybrid wind-diesel (IHWD) power system is widely used to generate the electricity on distant and isolated locations where the power grid is not available such as an island, offshore and mountain, *etc*. From the result of previous studies, such these areas should be sufficient to produce energy from wind [1–3]. In this research, the wind turbine generators (WTG) is combined with diesel generating (DG) sets to provide IHWD system for electricity generation. The main objective of combining the wind turbines with the diesel generating sets is to lower diesel fuel consumption, provide higher cost benefit for fossil fuels usage, and yield better environment. Nevertheless, intermittent wind input characteristics and various load changes can result in fluctuation of frequency and power [4, 5]. To overcome this problem, the load frequency control (LFC) uses the effective controllers to stabilize oscillations and maintain the frequency of the system so that they vary within an acceptable range.

There are several proposed controller designs for LFC system that help stabilize frequency oscillation, such as lead-lag controllers [6], proportional-integral controllers [7, 8], variable structure control [9,10], H∞ control [11] and fuzzy logic control [12–14].

However, the time response of the system using these controllers may be quite slow for compensating the load changes. Thus, in order to improve its response, the superconducting magnetic energy storage (SMES) [15–17] has been proposed in order to control the reactive and active power simultaneously [18, 19]. Besides, the SMES can gives additional benefit for a power quality improvement [20], a load levelling [21] and automatic generation control (AGC) problem or control of load frequency [22, 23].

Conventionally, LFC controllers are designed by using trial-and-error processes or the designer can use their experiences to design the system. At present, modern techniques that have been used to control LFC system are as follows: heuristic optimization such as multiple tabu search (MTS) [24], particle swarm optimization (PSO) [25], quasi-oppositional harmony search (QOHS) algorithm [26–31] and bee algorithm (BA) [32, 33] and *etc*.

This research concentrates on the bee algorithm (BA) to design optimal controllers *i.e.* PID controllers, SMES controllers and SF-FLPID controller for controlling the load frequency of an IHWD power system. Without using trial-and-error, the parameters of these controllers can easily be tuned by BA. For the results of simulation based on an IHWD system, the proposed optimal controllers can yield the excellent results when comparing in terms of the overshoot, the robustness, the time response, the settling time, and the performance index against various load changes in diesel side or/and input changes in wind side.

2. IHWD SYSTEM MODELING

Figure 1 demonstrates an IHWD power system with controllers.

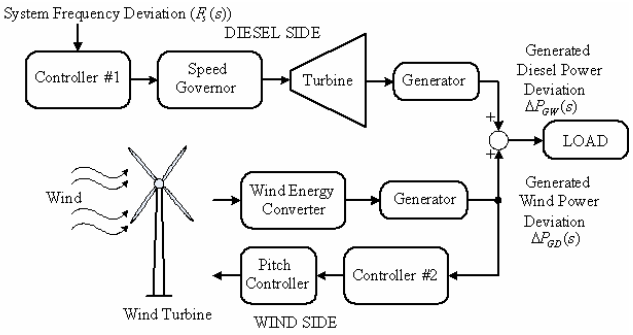

Fig. 1 – IHWD power system configuration.

For the DG unit, the governor performance of the generating unit can be improved by using controller # 1.

[1]Department of Electrical and Computer Engineering, Faculty of Engineering, Mahasarakham University, Mahasarakham 44150, Thailand, E-mail: srisuwan_w@yahoo.com

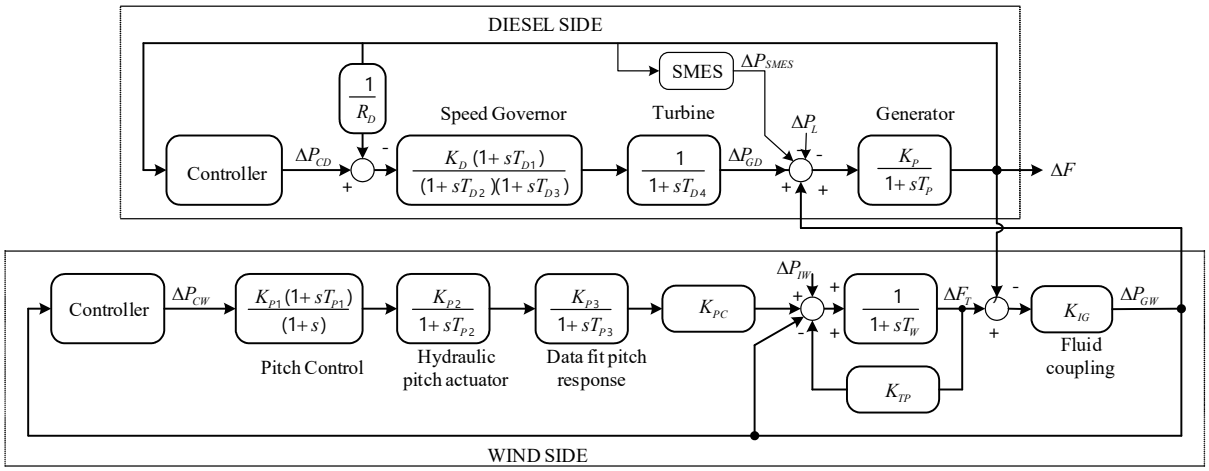

Fig. 2 – IHWD power system with frequency controllers and mathematic model [34].

The frequency deviation (ΔF) is assigned as a feedback signal. The controller can offset load demand by changing the speed-changer position and can offset the mismatch occurred in power generation. In the WTG units, controller # 2 is designed to control the pitch position. In the wind power generation, the occurred deviation is assigned as the input signal to maintain the stable generation. This IHWD system has the block diagram shown in Fig. 2.

The IHWD system which combined with SMES comprises of WTG, DG, and SMES devices. The studied IHWD has the system parameters shown in the Appendix. In this model, the power and frequency deviations are limited by the controller # 1 in DG, controller # 2 in WTG and SMES.

The incremental change of total output power ΔP_{total} can be calculated by. (1).

$$\Delta P_{total} = \Delta P_{GD} + \Delta P_{GW} - \Delta P_{SMES} - \Delta P_L , \quad (1)$$

where ΔP_{GD} is DG output power deviation, ΔP_{GW} is WTG output power deviation, ΔP_{SMES} is SMES output power deviation and ΔP_L is input load demand deviation.

2.1 WIND TURBINE GENERATOR

The characteristic of WTG is described in [31]. Normally, these characteristics are introduced as non-linear. However, the WTG can be written in term of the first-order systems which are represented in Eqs.(2)–(6).

$$\Delta F = \left(\frac{K_p}{1+sT_p}\right)\left[\Delta P_{GD} + \Delta P_{GW} - \Delta P_{SMES} - \Delta P_L\right], \quad (2)$$

$$\Delta P_{GW} = K_{IG}\left[\Delta F_T - \Delta F\right], \quad (3)$$

$$\Delta F_T = \left(\frac{1}{1+sT_W}\right)\left[K_{TP}\Delta F_T - \Delta P_{GW} + K_{PC}\Delta X_3 + \Delta P_{IW}\right], \quad (4)$$

$$\Delta X_3 = \Delta P_{CW}\left[\frac{K_{P1}K_{P2}K_{P3}(1+sT_{P1})}{(1+s)(1+sT_{P2})(1+T_{P3})}\right], \quad (5)$$

$$\Delta P_{CW} = \{TF\ of\ Controller\#2\}\left(\Delta P_{GW} - \Delta P_{GW(\max)}\right), \quad (6)$$

where K_{IG} is gain for the fluid coupling, K_{PC} is gain for the blade characteristic, K_{P1} is gain for the pitch control, K_{P2} is gain for the hydraulic pitch actuator, K_{P3} is gain for the data fit pitch response, T_{P1} is the time constant of the pitch controller, T_{P2} is the time constant of the hydraulic pitch actuator and T_{P3} is the time constant of the data fit pitch response.

2.2 DIESEL GENERATOR

In this model, the DG modelled by a 1st order transfer function can be represented by (7)–(10).

$$\Delta P_{GD} = \left(\frac{1}{1+sT_{D4}}\right)\Delta P_{GT} , \quad (7)$$

$$\Delta P_{GT} = \left(\frac{K_{D1}(1+sT_{D1})}{(1+sT_{D2})(1+sT_{D3})}\right)\Delta P_G , \quad (8)$$

$$\Delta P_G = \Delta P_{CD} - \frac{1}{R_D}\Delta F , \quad (9)$$

$$\Delta P_{CD} = \frac{1}{\Delta F}\{TF\ of\ Controller\#1\}, \quad (10)$$

where K_{D1} is gain for the speed governor, T_{D1}, T_{D2}, T_{D3} are the speed governor time constants, T_{D4} is the speed governor time constants. Thus, the value of ΔP_{GD}, as involved in (1), may be calculated.

3. FREQUECY CONTROLLER

3.1 PID CONTROLLER

The most popular controller in the process industry is the PID controller. It has been used successfully for over 50 years. The PID controller has the advantage of being robust, easy to work with, and excellent control efficiency, despite the varying dynamic characteristics of the process plant.

The PID controller consists of three parameters, the most popular controller in the process industry is the PID controller. It has been used successfully for over 50 years. The PID controller has the advantage of being robust, easy to work with, and excellent control efficiency, despite the varying dynamic characteristics of the process plant. The PID controller consists of three parameters, the proportional gain (k_p), the integral gain (k_i) and the derivative gain (k_d). For PID controller design, these gains are tuned by trial and error based on the experienced designer. The effects of these gains on the system are:

Proportional gain:
- Reduce the rise time and settling time.
- If it is too high, the system may be unstable.
- If it is low, the time response is slow
- It does not eliminate the steady state error.

Integral gain:
- Eliminate the steady-state error.
- If it is high, increase the overshoot.
- If it is low, the time response is slow.

Derivative gain:
- Increase system stability
- Reduce overshoot
- Improve transient response.
- If it is too high, the system may be unstable.

The transfer function of the PID controller is shown in Fig. 3 [29].

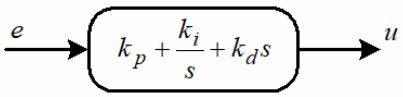

Fig. 3 – Block diagram of PID controller.

The input signal is an error (e).The control signal u is calculated by

$$u = \left(k_p + \frac{k_i}{s} + k_d s \right) e . \quad (11)$$

In designing the optimal PID controller, the controller gains (k_p, k_i and k_d) are determined by BA.

3.2 SF-FLPID CONTROLLER

The SF-FLPID controller comprises of three components *i.e.* scaling factor (SF), fuzzy logic (FL) and PID controllers which all of them are connected in series. The SF-FL controller has been chosen since it has fixed predefined the MFs and CR (shown in Fig. 4, as used for this study) of FL controller. For designing the SF-FL controller, the accuracy of SF has the highest priority because of the effect of their value on the performance of controller. However, a crucial relation between the input SFs and the performance of a FL controller has not been completely established. Therefore, the PID controllers have been hybridized with the SF-FL controller such that the hybridized controller may be categorized as SF-FLPID controller. The SF-FLPID controller structure used in the current study is shown in Fig. 5. [29].

The main procedure in designing the optimal SF-FLPID controller is the method to estimate the scaling factor gains (k_1 and k_2) and PID controller gains (k_p, k_i and k_d). In general, we can use the trial and error process and the designer experiences to estimate these gains. However, this paper solves this issue by applying BA to determine these gains.

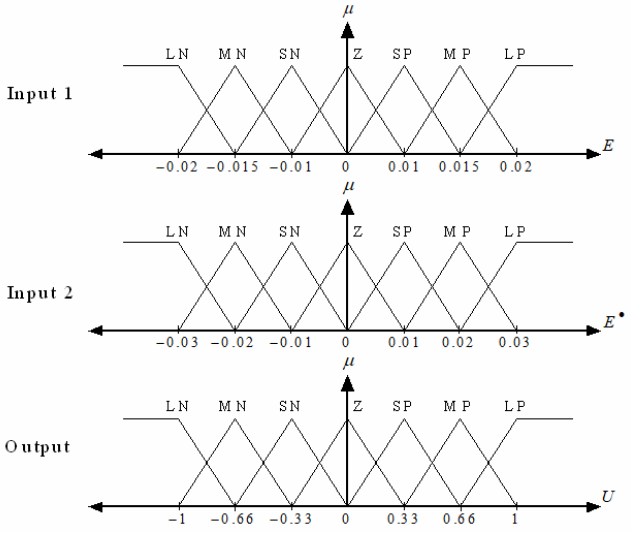

LN: large negative; MN: medium negative; SN: small negative;
Z: zero; SP: small positive; MP: medium positive;
LP: large positive.

(a) Membership functions

E \ E•	LN	MN	SN	Z	SP	MP	LP
LN	LP	LP	LP	MP	MP	SP	Z
MN	LP	MP	MP	MP	SP	Z	SN
SN	LP	MP	SP	SP	Z	SN	MN
Z	MP	MP	SP	Z	SN	MN	MN
SP	MP	SP	Z	SN	SN	MN	LN
MP	SP	Z	SN	MN	MN	MN	LN
LP	Z	SN	MN	MN	LN	LN	LN

(b) Control rules

Fig. 4 – Membership function and control rule for SF-FLPID controller.

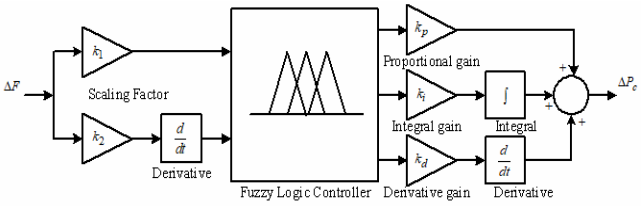

Fig. 5 – Structure of proposed SF-FLPID controller.

3.3 SMES CONTROLLER

Under load changes, the SMES controller is used to stabilize and damp out the low-frequency oscillation of the system. The structure of the SMES controller is displayed

in Fig. 6. The SMES has the transfer function represented by [27]

$$\Delta P_{SMES} = K_F \times \left(\frac{1+sT_1}{1+sT_2}\right) \times \left(\frac{1+sT_3}{1+sT_4}\right) \times \left(\frac{K_{SMES}}{1+sT_{SMES}}\right) \times \Delta F_s, \quad (12)$$

where K_{SMES}, T_{SMES} and T_1, T_2, T_3 and T_4 are gain and time constants (in second) of the SMES, respectively.

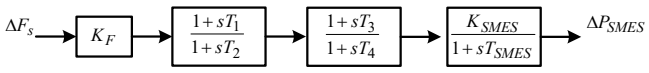

Fig. 6 – Structure of SMES as frequency stabilizer

In designing the SMES controller, the parameter K_F has been fixed and the parameters (K_{SMES}, T_{SMES}, T_{SMES}, T_1, T_2, T_3 and T_4) are determined by BA.

4. BEE ALGORITHM

In 2005, D.T. Pham [35] first proposed the BA to solve the optimization numerical problems. As an artificial optimization algorithm, the BA approach can imitate the behaviour of honey bees when they forage food in the natural environment. To find out the good food source, honey bees use a reference point (the sub) for navigation and communication (waggle dance in the hive). Therefore, the honey bees' behaviour can be applied to develop a new optimization algorithm which is simple, effective and robust for searching optimum solution. Typically, a honey bee colony comprises of 3 groups of adult bees: workers, drones, and a queen. Many thousand bees that are workers have worked together in building nest, collecting food, and rearing brood. The BA approach considers only the worker bees and separates the worker bees into 2 types: employed and scout bees. The scout bee has responsibility to survey the new expected food sources and come back to the hive for information sharing to other bees in the hive. After that, the employed bee has responsibility to find out the good food sources, memorize the best food source, and share the search information to other bees.

The procedures of applying BA to design the optimal PID, SF-FLPID and SMES controllers are described as follow:

N is number of iterations,

$N_{\max}$ is maximum iterations,

n_s is number of scout bees,

m_s is number of best selected sites out of n_s visit sites,

e_s is number of best selected sites out of m_s selected sites,

n_{ep} is number of employed bees recruited for the e_s best sites,

n_{sp} is number of employed bees recruited for other $(m_s - e_s)$ selected sites,

n_{size} is neighborhood size,

Step 0: (initial step)

- Determine the values of $N_{\max}$, n_s, m_s, e_s, n_{ep} and n_{sp}.
- Determine the minimum and maximum values of each tuned parameters.
- Set initial iteration $N = 0$.

Step 1: Generate random initial solutions (n_s) of scout bees for tuned parameters. These initial solutions must be feasible candidate solutions that satisfy constraints.

Step 2: Represent the values of the solutions into the controllers. Simulate the system model in order to find the time response of ΔF_s correspond to the time t.

Step 3: Evaluate the objective function by substituting ΔF_s and t into equation (13). Arrange the solution according to the objective values from the best to worst values.

Step 4: Select the m_s best selected solutions out of n_s solutions for neighborhood search. Separate the m_s best selected solutions into two groups, the first group has the e_s best selected solutions and another group has the $(m_s - e_s)$ best selected solutions.

Step 5: Generate the random neighborhood size (n_{size}) of each the best selected solutions.

Step 6: Generate random neighborhood solutions n_{ep} and n_{sp} of the e_s best selected solutions and the $(m_s - e_s)$ best selected solutions, respectively.

Step 7: Represent the values of the neighborhood solution into the controllers. Simulate the system model in order to find the time response of ΔF_s correspond to the time t.

Step 8: Evaluate the objective function by substituting ΔF_s and t into equation (13). Arrange the neighborhood solutions of each site according to the objective values from the best to worst values.

Step 9: Select the best solution of each site.

Step 10: Check the stopping criterion. If satisfied, stop the search, else set $N = N + 1$.

Step 11: Generate new random solutions ($n_s - m_s$) of scout bees for the tuned parameters. Combine the existing (m_s) and the new solutions ($n_s - m_s$) as the solution (n_s) for next iteration. Go to Step 2.

5. NUMERICAL RESULTS

The following controllers are designed individually for comparison studies.

1. Optimal PID controller,
2. Optimal SF-PLPID controller,
3. Optimal PID with SMES controllers.
4. Optimal SF-FLPID with SMES controllers.

Matlab2016-Simulink and fuzzy-logic toolbox are used for performing the simulation on the laptop computer (Intel 2.20 GHz, Core i5-5200u, Ram 4 GB, OS: Windows 8).

Below is the objective function (J) in which the performance index is the integral of time-multiplied absolute error (ITAE)

$$\text{Minimize } J = \int_0^5 t\left|\Delta F_s\right| \mathrm{d}t \ . \quad (13)$$

Simulation results under 5 case studies are carried out as follows.

Case 1: Step input of load change on diesel side

First, the diesel side is fed with 0.01 p.u. step load disturbance at t = 0 s. As a result, four controllers have the tuned parameters displayed in Table 1. In Fig. 7, the system

frequency deviations after an abrupt load change are displayed. The simulation results can evaluate the significant transient performance values i.e. settling time (T_s), steady state error (E_{ss}), overshoot (O_{sh}), undershoot (U_{sh}) and ITAE of frequency deviation (shown in Fig. 7 and Table 2).

Table 1
The tuned parameters of controllers ($\Delta P_L = 0.01$ and $\Delta P_{IW} = 0$)

System side	Parameters	Controller			
		PID	SF-PID	PID + SMES	SF-FLPID + SMES
Diesel	$K_{1\text{-}d}$	-	2.74	-	2.45
	$K_{2\text{-}d}$	-	2.49	-	2.72
	$K_{p\text{-}d}$	213.18	1.16	101.00	1.07
	$K_{i\text{-}d}$	35.43	0.30	89.03	0.60
	$K_{d\text{-}d}$	16.70	0.00	14.60	0.00
Wind	$K_{1\text{-}w}$	-	0.30	-	0.29
	$K_{2\text{-}w}$	-	0.55	-	0.11
	$K_{p\text{-}w}$	5.785	0.34	42.77	0.06
	$K_{i\text{-}w}$	34.56	0.12	35.29	0.00
	$K_{d\text{-}w}$	9.25	0.08	12.84	0.24
SMES	K_{SMES}	-	-	2.45	3.20
	T_{SMES}	-	-	0.04	0.01
	T_1	-	-	4.48	4.76
	T_2	-	-	4.01	4.05
	T_3	-	-	0.09	0.09
	T_4	-	-	4.65	4.69

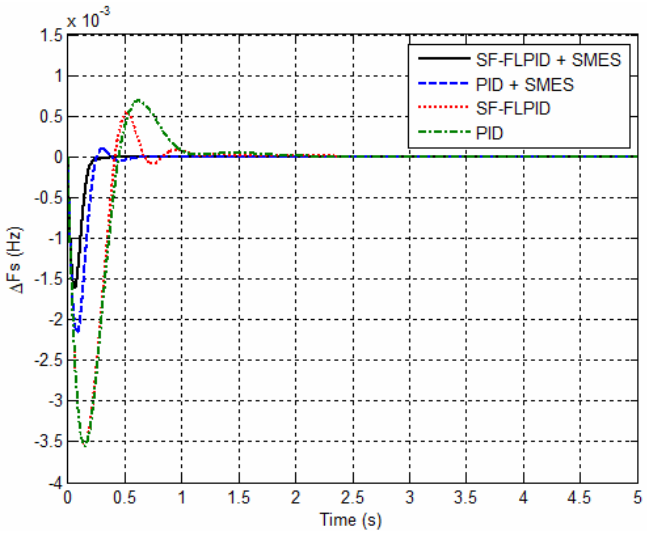

Fig. 7 – Time response of ΔF_s ($\Delta P_L = 0.01$ and $\Delta P_{IW} = 0$).

Table 2
Performance values of frequency deviation in Case 1.

Controllers	Performance values				
	T_s (s)	E_{ss} ($\times 10^{-6}$)	O_{sh} ($\times 10^{-3}$)	U_{sh} ($\times 10^{-3}$)	ITAE ($\times 10^{3}$)
PID	1.0069	-2.4484	0.6855	-3.5524	0.4027
SF-FLPID	1.0138	-4.3311	0.5483	-3.5255	0.2774
PID+SMES	0.5080	-3.3241	0.1009	-2.1559	0.0574
SF-FLPID+ SMES	0.2360	-0.3285	0.0002	-1.6193	0.0171

Case 2: Step input of load change on wind side

In this case, the wind side was fed with 0.01 pu. step load disturbance at t = 0 second. As a result, four controllers have the tuned parameters displayed in Table 3. For Fig. 8., it shows the system frequency deviations after an abrupt load change. The transient performance values *i.e.* T_s, E_{ss}, O_{sh}, U_{sh} and ITAE of frequency deviation are shown in Fig. 8 and Table 4.

Table 3
The tuned parameters of controllers ($\Delta P_L = 0$ and $\Delta P_{IW} = 0.01$)

System side	Parameters	Controller			
		PID	SF-PID	PID + SMES	SF-FLPID + SMES
Diesel	$K_{1\text{-}d}$	-	2.79	-	3.83
	$K_{2\text{-}d}$	-	2.70	-	1.12
	$K_{p\text{-}d}$	296.58	1.59	227.20	2.80
	$K_{i\text{-}d}$	68.22	1.60	74.85	2.04
	$K_{d\text{-}d}$	81.80	0.00	48.23	0.11
Wind	$K_{1\text{-}w}$	-	0.54	-	-0.28
	$K_{2\text{-}w}$	-	0.34	-	-0.14
	$K_{p\text{-}w}$	55.72	0.04	70.82	-0.00
	$K_{i\text{-}w}$	3.06	0.00	9.87	-0.00
	$K_{d\text{-}w}$	133.80	0.06	161.66	0.45
SMES	K_{SMES}	-	-	9.58	4.68
	T_{SMES}	-	-	2.67	0.70
	T_1	-	-	1.36	7.37
	T_2	-	-	5.37	5.93
	T_3	-	-	7.48	0.06
	T_4	-	-	6.61	7.08

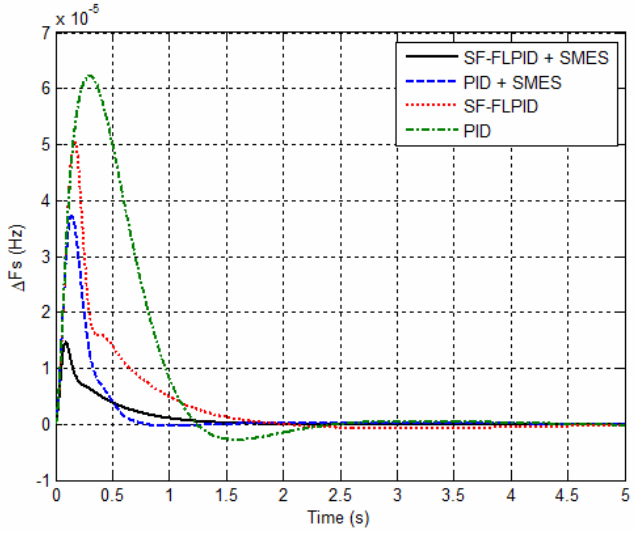

Fig. 8 – Time response of ΔF_s ($\Delta P_L = 0$ and $\Delta P_{IW} = 0.01$).

Table 4
Performance values of frequency deviation in Case 2.

Controllers	Performance values				
	T_s (s)	E_{ss} ($\times 10^{-6}$)	O_{sh} ($\times 10^{-5}$)	U_{sh} ($\times 10^{-5}$)	ITAE ($\times 10^{3}$)
PID	2.0806	-0.2157	6.2299	-0.2807	0.0022
SF-FLPID	1.5543	-0.2498	5.0567	-0.0803	0.0138
PID+SMES	0.6663	-0.0332	3.7221	-0.0369	0.0034
SF-FLPID+ SMES	1.4078	-0.0065	1.4792	-0.0022	0.0020

Case 3: Step input of load change on both sides

In this case, diesel and wind sides are fed with 0.01 pu. step load disturbances at t = 0 second. As a result, four controllers have the tuned parameters displayed in Table 5.

The system frequency deviations after an abrupt load change are displayed in Fig. 9. The transient performance values *i.e.* T_s, E_{ss}, O_{sh}, U_{sh} and ITAE of frequency deviation, presented in Fig. 8, are featured in Table 6.

Table 5
The tuned parameters of controllers ($\Delta P_L, \Delta P_{IW} = 0.01$)

System side	Parameters	Controller			
		PID	SF-PID	PID + SMES	SF-FLPID + SMES
Diesel	$K_{1\text{-}d}$	-	2.74	-	5.97
	$K_{2\text{-}d}$	-	3.08	-	3.23
	$K_{p\text{-}d}$	235.94	1.07	22.94	1.13
	$K_{i\text{-}d}$	8.87	1.50	65.13	1.61
	$K_{d\text{-}d}$	14.54	0.00	17.81	0.00
Wind	$K_{1\text{-}w}$	-	0.15	-	0.10
	$K_{2\text{-}w}$	-	0.61	-	0.41
	$K_{p\text{-}w}$	-31.46	0.07	28.74	0.16
	$K_{i\text{-}w}$	2.72	0.13	3.69	0.20
	$K_{d\text{-}w}$	68.03	0.11	15.01	0.19
SMES	K_{SMES}	-	-	9.47	10.02
	T_{SMES}	-	-	0.94	0.07
	T_1	-	-	1.93	1.00
	T_2	-	-	7.33	4.36
	T_3	-	-	3.31	3.96
	T_4	-	-	9.43	10.90

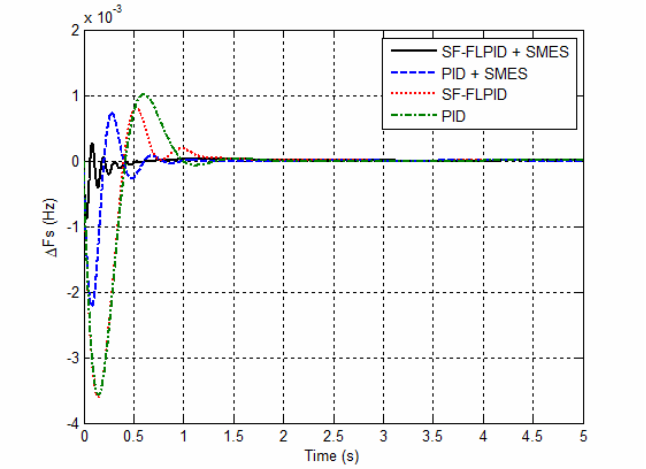

Fig. 9 – Time response of ΔF_s ($\Delta P_L, \Delta P_{IW} = 0.01$).

Table 6
Performance values of frequency deviation in Case 3.

Controllers	Performance values				
	T_s (s)	E_{ss} ($\times 10^{-6}$)	O_{sh} ($\times 10^{-3}$)	U_{sh} ($\times 10^{-3}$)	ITAE ($\times 10^{3}$)
PID	0.9510	11.4190	1.0104	-3.5635	0.4687
SF-FLPID	1.1539	1.6202	0.8015	-3.6032	0.3295
PID+SMES	0.7415	-0.1979	0.7253	-2.2227	0.0822
SF-FLPID+ SMES	0.6537	-0.0724	0.2723	-0.8924	0.0566

Case 4: Random input of load change on both sides

The random step load disturbances are applied to diesel side (displayed in Fig. 10(a)) and the random sinusoidal load disturbances (shown in Fig. 10(b)) are applied to wind side at t = 0 to t = 50 s. The tuned parameters of 4 controllers in Table 5 are tested in this case.

The system frequency deviations after changing the load randomly are shown in Fig. 11.

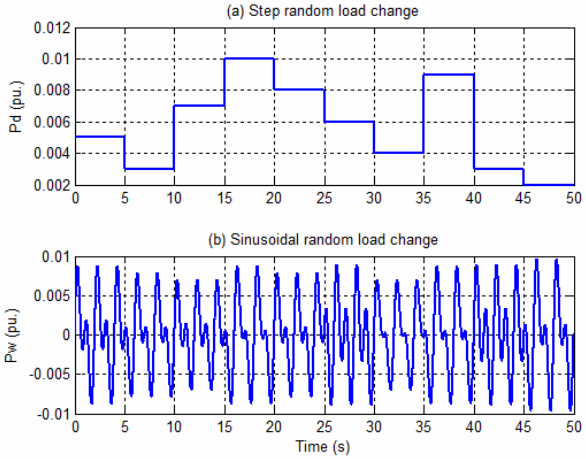

Fig. 10 – Step and sinusoidal random load change.

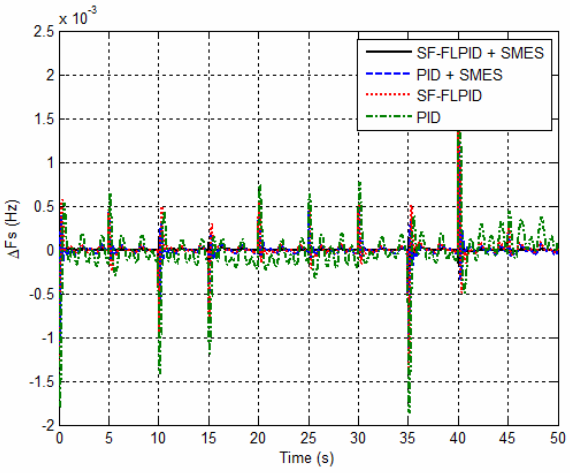

Fig. 11 – Time response of ΔF_s under random load change

Case 5: System parameters variation

Next, controller robustness versus system parameters variations is estimated with performance index, overshoot, and settling time and they will be computed when the 0.01 p.u. step load changes are fed on both sides while all system parameters have the nominal values varied between –0 and 30 . The results of comparison are shown in Figs. 12 –14 in which the values of performance index, overshoot, and settling time of the frequency variation of the system are displayed respectively.

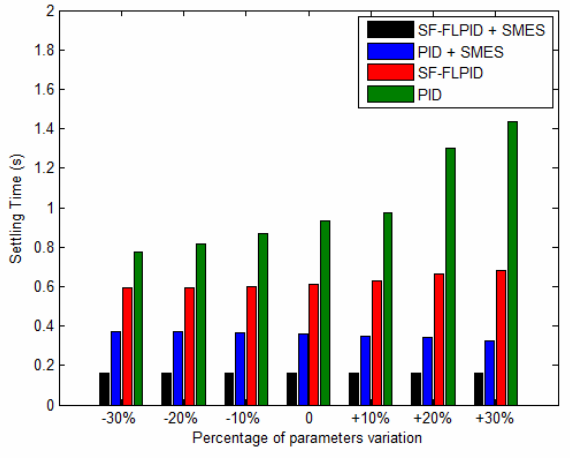

Fig. 12 – Comparison results of settling time of ΔF_s.

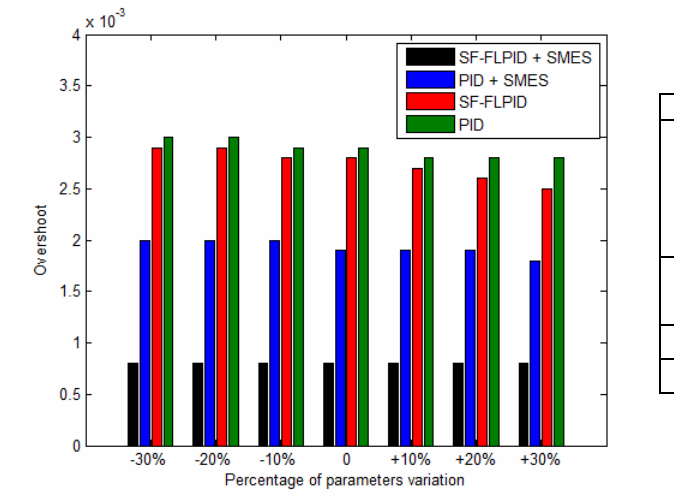

Fig. 13 – Comparison results of overshoot of ΔF_s.

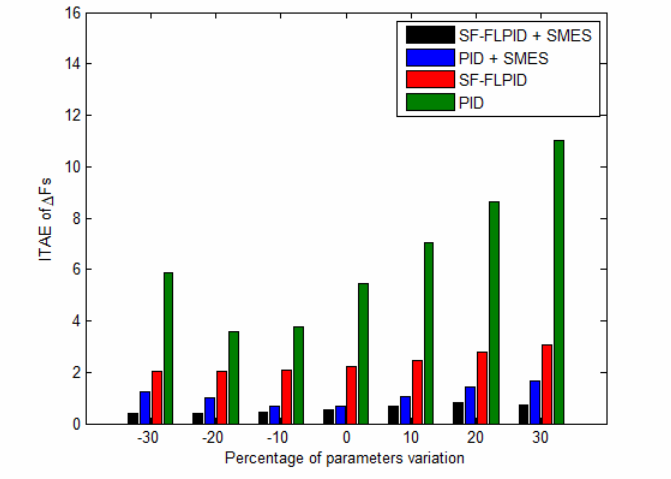

Fig. 14 – Comparison results of ITAE of ΔF_s.

Considering Figs 12 –14, these clarify that the optimal SF-FLPID controller robustness compared to the variations of parameters is better than that of the other controllers.

6. CONCLUSIONS

In this research paper, the BA has been applied to design an optimal PID, SF-FLPID and SMES controllers that can control the load frequency of an IHWD power system. The benefits of this proposed approach include ease of implementation, fast designing, good performance. In order to verify the effectiveness and robustness, the proposed PID, SF-FLPID and SMES controllers have also been tested with several case studies. In conclusion, simulation results prove that the proposed SF-FLPID including SMES controller can performs essentially better than other controllers in term of the settling time, overshoot, and performance index (ITAE).

Received on August 3, 2018

APPENDIX A

Table A.1

Model	Parameters		
Wind unit	$K_{p1} = 1.25$ $K_{PC} = 0.080$ $T_{P1} = 0.6\,\text{s}$ $T_w = 4\,s$	$K_{p2} = 1.00$ $K_{IG} = 0.9969$ $T_{P2} = 0.041\,\text{s}$	$K_{p3} = 1.40$ $K_{TP} = 0.0033$ $T_{P3} = 1\,\text{s}$
Diesel unit	$K_D = 0.3333$ $T_{D3} = 0.025\,\text{s}$	$T_{D1} = 1\,\text{s}$ $T_{D4} = 3\,\text{s}$	$T_{D2} = 2\,\text{s}$
SMES	$K_F = 50$		
Power system	$K_P = 72$	$T_P = 14.4\,\text{s}$	$R_D = 5$

Remark: The rated capacities of DG and WTG are 150 kW.

ACKNOWLEDGEMENT

We would like to express our special thanks of gratitude to Dr. Saravuth Pothiya and Prof. Dr. Issarachai Ngamroo for their guidance in completing our work.

REFERENCES

1. T.S Bhatti, A.A.F. AI-Ademi, N.K. Bansal, *Load frequency control of isolated wind diesel hybrid power system*, Energy Conver.Mgnt, **38**, *9*, pp. 829-837 (1997).
2. Z.M. Ai-Hamouz, Y.L. Abdel-Magid, *Variable-structure load-frequency controllers for multi area power systems*, Int. J. Electr. PowerEnerg. Syst., **15**, 5, pp. 23-29 (1993).
3. Y. Bendjeddou, R. Abdessemed, E. Merabet, L. Bentohami, *Fuzzy controller for self excited dual star induction generator with online estimation of magnetizing inductance used in wind energy conversion*, Rev. Roum. Sci. Techn. – Électrotechn. Et Énerg., **63**, *4*, pp. 417–422 (2018).
4. N. Kodama, T. Matsuzaka, N. Inomata, *The power variation control of a wind generator by using probabilistic optimal control*, Trans. Inst. Elect. Eng. Jpn., **121**, *1*, pp. 22–30 (2001).
5. H. Holttinen, R. Hirvonen, *Power system requirements for wind power*, John Wiley & Sons Ltd, 2005, Chapter 8.
6. N. Jaleeli, LS. VanSlyck, DN. Ewart, LH. Fink, AG. Hoffmann, *Understanding automatic generation control*, IEEE Trans Power Systems, **7**, *3*, pp. 1106-1112 (1992).
7. O.P. Malik, A. Kumar, G.S. Hope, *A load frequency control algorithm based on a generalized approach*, IEEE Trans. Power Syst., **3**, 2, (1988).
8. Antar Beddar, Hacene Bouzekri, Badreddine Babes, Hamza Afghoul, *Real time implementation of improved fractional order proportional-integral controller for grid connected wind energy conversion system*, Rev. Roum. Sci. Techn. – Électrotechn. Et Énerg., **61**, *4*, pp. 402–407 (2016).
9. A. Kumar, O.P. Malik, G.S. Hope, *Variable structure-system control applied to AGC ofan interconnected power system*, lEE, **132**, *1*, pp. 23-29 (1985).
10. Z.M. Ai-Hamouz, Y.L. Abdel-Magid, *Variable-structure load frequency controllers for multi area power systems*, Int. J. Electr. PowerEnerg. Syst., **15**, *5*, pp. 23-29 (1993).
11. I. Ngamroo, C. Taeratanachai, S. Dechanupaprittha, Y. Mitani, *Enhancement of load frequency stabilization effect of superconducting magnetic energy storage by static synchronous series compensator based on $H\infty$ control*, Energy Convers Manage; **48**, *4*, pp. 1302-1312 (2007).
12. H. Deboucha, S. Lalouni Belaid, *Improved incremental conductance maximum power point tracking algorithm using fuzzy logic controller for photovoltaic system*, Rev. Roum. Sci. Techn. – Électrotechn. Et Énerg., **62**, *4*, pp. 381–387 (2017).
13. J. Talaq, F. AL-Basri, *Adaptive fuzzy gain scheduling for load frequency control*, IEEE Trans. Power Systems, **14**, *1*, pp. 145-150 (1999).
14. S. Pothiya, I. Ngamroo, S. Runggeratigul, and P. Tantaswadi, *Design of optimal fuzzy logic based PI controller using multiple tabu search algorithm for load frequency control*, International Journal of Control, Automation, and Systems, **4**, *2*, pp. 155-164 (2006).
15. R.W. Boom, H. Perterson, *A superconducting energy storage for power systems*. IEEE Trans Magn, **8**, pp. 701-703 (1972).

16. W. Hassenzahl, *Will Superconducting magnetic energy storage be used on electric utility systems*. IEEE Trans Magn, **1**, pp. 482-488 (1975).
17. H.J. Boenig, J.F. Hauer, *Commissioning tests of the bonneville power administration 30 MJ superconducting magnetic energy storage unit*, IEEE Trans Power Appl Syst, **10**, pp. 302–309 (1985).
18. T. Ise, Y. Mitani, K. Tsuji, *Simultaneous active and reactive power control of superconducting magnetic energy storage to improve power system dynamic performance*, IEEE Trans Power Deliv, **1**, pp. 143-150 (1986).
19. B.C. Pal, A.H. Coonick, B.J. Cory, *Robust damping of inter-area oscillations in power systems with superconducting magnetic energy storage devices*, IEE Proc Gen Trans Distrib, **146**, *6*, pp. 633-639 (1999).
20. M.K. Abdelsalam, R.W. Boom, H.A. Perterson, *Operation aspects of superconducting magnetic energy (SMES)*, IEEE Trans Mag, **23**, pp. 3275-3277 (1987).
21. X. Chu, X. Jiang, Y. Lai, X. Wu, W. Liu, *SMES control algorithms for improving customer power quality*, IEEE Trans Appl Super , **11**, *1*, pp. 1769-1772 (2001).
22. S.C. Tripathy, R. Balasubramanian, P.S. Chandramohanan Nair, *Adaptive automatic generation control with superconducting magnetic energy storage in power systems*, IEEE Trans Energy Conv, **7**, 3, pp. 434-441 (1997).
23. A. Demiroren, H.L. Zeynelgil, N.S. Sengor, *Automatic generation control for power system with SMES by using neural network controller* Electr Power Comp Syst, **31**, *1*, pp. 1-25 (2003).
24. S. Pothiya, I. Ngamroo, *Optimal fuzzy logic-based PID controller for load frequency control including superconducting magnetic energy storage units*, Energy Conversion and Management, **49**, *10*, pp. 2833-2838 (2008).
25. S. Anbarasi, S. Muralidharan, *Intelligent tuning of proportional integral derivative controller using hybrid bacterial foraging particle swarm optimization for automatic voltage regulator system*, Rev. Roum. Sci. Techn. – Électrotechn. Et Énerg., **62**, *3*, pp. 325–331 (2017).
26. M. Tarkeshwar, V. Mukherjee, *Quasi-oppositional harmony search algorithm and fuzzy logic controller for load frequency stabilization of an isolated hybrid power system*. IET Gener. Transm. Distrib., **9**, *5*, pp. 427-444 (2015).
27. M. Tarkeshwar, V. Mukherjee, *A novel quasi-oppositional harmony search algorithm and fuzzy logic controller for load frequency stabilization of an isolated hybrid power system*, Electrical Power and Energy Systems, **66**, pp. 247-261 (2015).
28. T. Mahto, V. Mukherjee, *Evolutionary optimization technique for comparative analysis of different classical controllers for an isolated wind–diesel hybrid power system*, Swarm and Evolutionary Computation, **26**, pp. 120–136 (2016).
29. T. Mahto, V. Mukherjee, *A novel scaling factor based fuzzy logic controller for frequency control of an* isolated *hybrid power system*, Energy, **130**, pp. 339-350 (2017).
30. T. Mahto, V. Mukherjee, *Fractional order fuzzy PID controller for wind energy-based hybrid power system using quasi-oppositional harmony search algorithm*, IET Gener. Transm. Distrib, **11**, *13*, pp. 3299-3309 (2017).
31. S. Ganguly, T. Mahto, V. Mukherjee. *Integrated frequency and power control of an isolated hybrid power system considering scaling factor based fuzzy classical controller*, Swarm and Evolutionary Computation, **32**, pp. 184–201 (2017).
32. T. Chaiyatham, I. Ngamroo, S. Pothiya, S. Vachirasricirikul, *Fuzzy logic PID based SMES controller design using Bee Colony Optimization for stabilization of inter-area oscillation*, IEEE ECTI-CON conference, 2009.
33. P. Durongdumrongchai, W. Sa-Ngiamvibol, A. Aurasopon, S. Pothiya, *Robust and optimal fuzzy logic proportional-integral-derivative controller design by bee algorithm for hydro-thermal system*, Rev. Roum. Sci. Techn. – Électrotechn. Et Énerg., **59**, *2*, pp. 193-203 (2014).
34. T.S. Bhatti, A.A.F. Al-Ademi, N.K. Bansal, *Load frequency control of isolated wind diesel hybrid power systems*, Energy Convers. Manag., **38**, *9*, pp. 829–837 (1997).
35. D.T. Pham, A. Ghanbarzadeh, E. Koc, S. Otri, M. Zaidi, *The bees Algorithm*, Technical Note, Manufacturing Engineering Centre, Cardiff University, UK (2005).